Article

Effects of Soil–Rock Geomorphic Units on the Yield of Surface Runoff: A Case Study on Uncultivated Land of a Karst Area

Zhimeng Zhao [1,*], Qinghe Wang [2,3] and Jin Zhang [3,4]

1. Guizhou Provincial Key Laboratory of Geographic State Monitoring of Watershed, School of Geography and Resources, Guizhou Education University, Guiyang 550018, China
2. Xishuangbanna Tropical Botanical Garden, Chinese Academy of Sciences, Kunming 650221, China; wangqinghe@xtbg.ac.cn
3. University of Chinese Academy of Sciences, Beijing 100049, China; zhangj@ucas.ac.cn
4. School of Mathematical Sciences, Chinese Academy of Sciences, Beijing 100049, China
* Correspondence: zhaozhimeng@gznc.edu.cn

Abstract: Surface runoff on karst is a multifactorial hydrological process. There are a great number of studies focusing on rainfall–runoff from karst slopes on a large scale, but microscale studies related to soil–rock geomorphic units have been rarely reported. This study used rock–soil runoff plots on uncultivated land as a new form of natural rainfall catchment, and the yield of surface runoff was measured during four different rainfall events. Through monitoring rainfall runoff by soil–rock runoff plots under different rainfall events, it has been proven that the coefficient of surface runoff measured on uncultivated land of a karst area is very small compared to that of non-karst areas, only ranging from 0.0145 to 0.0408 in the measurement period. And multiple regression analysis showed that the rocks contributed less to the yield of surface runoff than the soils, and with the increase in rainfall, the contributions of both showed an increasing trend. The calculated surface runoff yield produced by soils showed a positive relationship with soil bulk density and a negative relationship with soil porosity, soil hydraulic conductivity, and root biomass, and the significance increased with rainfall, which was consistent with previous findings and demonstrated the accuracy and efficiency of the proposed method in our study. These study results contribute to a deeper understanding of the rainfall–runoff process in rocky desertification areas, and the proposed method of soil–rock runoff plots provides a new way to estimate the yield of rainfall runoff on the complicated geomorphic units of karst slopes.

Keywords: rainfall–runoff process; runoff yield; water loss; rocky karst area; soil–rock geomorphic unit

1. Introduction

Water loss into underlying rocks is one of the important factors limiting ecological restoration in karst areas, and its impact on agriculture has seriously restricted the social and economic development of these regions [1–4]. Water resources in a karst area are so reduced that even essentials such as drinking water for people and livestock are difficult to find. A karst area is widely recognized as a typical fragile ecological environment, because agricultural land is scarce, productivity is sharply reduced, and the ecosystem is unstable [5–7]. Karst hydrology is a complex subject to study; however, the atmosphere–biology–soil–water–rock continuum in the karst zone is the basis for understanding the structure, process, and function of the karst ecosystem [8–10]. This paper provides a theoretical basis for understanding hydrological processes in karst areas by using a new way, soil–rock runoff plots, to quantify the effects of aboveground rocks and soils on the surface runoff yield in small-scale geomorphic units.

Water is the lifeblood of karst vegetation [11,12]. Plants growing in karst areas are frequently affected by many environmental factors, but in karst areas, water is undoubtedly

the most important growth-limiting factor among them [13,14]. The karst area studied is located in the monsoon zone of the subtropics in southwest China where abundant rainfall provides the natural conditions for karst development [15,16]. Due to dissolution by rainfall, the bedrock has undergone strong karstification, and the landscape has developed a spatial duality between surface and underground hydrogeological structures [17–19]. In karst rocky desertification areas, the soil cover on the surface is characteristically thin and discontinuous with weak waterholding capability, so the conversion of surface water to groundwater is rapid [20,21]. Therefore, although the region has abundant rainfall, the water easily infiltrates into underground systems through the soil, as well as through fissures and conduits [22–25]. A part of the rainwater intercepted by the rocks quickly seeps through as preferential flow, and another part is transferred to the surrounding soil, but researchers newly found that this flow behavior varies widely, and its effect on karst hydrology and surface runoff in particular is unclear [4,26–28]. In general, the karst landform contributes less to surface runoff, and this causes a temporary drought in the surface soil and a serious shortage of water for agricultural irrigation. Water is the key to solving the area's problems, and it is therefore important to study the processes and characteristics of water movement in karstic rocky desertification areas [29–31]. However, the current research on karst hydrology generally pays attention to the large scale, such as a region or watershed [32–34], and there are few reports on a microscale, especially on soil–rock combination microgeomorphic units, and the contribution of soil and rock to surface runoff is unclear.

The spatial characteristic of soil water loss in the karst area is strongly tied to the geological environment, and the ecological processes there often show significant differences from other types of ecosystems [35–37]. In the rocky desertification area, the surface soil is shallow, and the exposed area of bedrock is commonly high, limiting the water storage capacity of the soil. And moreover, rock outcrops as the main surface element commonly increase the complexity and heterogeneity of water distribution and movement [38–40]. Studies of the influence of bare rock on soil water content have shown that exposed rocks in this part of southwest China can affect the water content of soil patches adjacent to them during the rainy season. When the rock coverage reaches 70%, the water coming from the rocks is equal to the precipitation received by the soil patches, which means that the water supply obtained by the soil patches is twice the precipitation [38,41]. More importantly, the water accumulation adjacent to the rocks is greater than in areas without rocks, thus forming sites that are relatively conducive to vegetation restoration [40–42]. In addition, rock outcrops have an effect on the surface runoff of the karst slopes, which greatly depends on the orientation of the rocks. The rocks parallel to the slope leave a flow channel for surface runoff, whereas the transverse rocks hinder it and reduce the flow velocity [27,43]. These latest findings explain why there are always differences in the hydrological research results from different karst areas. Aside from the rocks, surface runoff from karst slopes is also subject to the influence of many other factors, for example, water infiltration in soils varying with the soil particle composition, soil permeability, and soil water content [28,44,45]. And vegetation litter and well-developed root systems can change the rates of surface runoff and the recharge of groundwater by reducing soil density [28,46,47]. Surface runoff from karst slopes is, therefore, a multifactorial hydrological process, which is an important part of the conversion from surface water to groundwater, and surface runoff and water infiltration within the special karst geographic background should be taken into consideration when designing water management for crops. Nevertheless, the relationship between the rock–soil geomorphic units and surface runoff has not been fully resolved, which seriously affects the research on the mechanism of soil and water loss in karst areas.

The karstic area of China covers approximately 3.44 million km^2, accounting for 1/3 of the total land area, of which southwest China contains approximately 0.54 million km^2. The area is well known as the largest karst ecosystem in the world, with 0.12 million km^2 of land with rocky desertification [48]. Guizhou province is a famous karst area, providing ideal conditions to fully study the contribution of karst to runoff and analyze the migration

and generation characteristics of rainfall–runoff under various geomorphic units. However, in the past, most of the research on karst surface runoff is usually based on traditional slope-scale runoff plots. This study selected different soil–rock combinations on uncultivated land as natural rainfall catchment units, and the yield of surface runoff was measured using a new way of soil–rock runoff plots under different rainfall events. The contribution of the selected soil–rock combinations on runoff yield was then analyzed. This study can provide the theoretical support needed for technological research and development of water loss prevention and control on karst slopes.

2. Materials and Methods

2.1. Study Site

This experiment was conducted on a severe rocky desertification farmland plot (26°57′23″ N, 106°6′21″ E) in Makan Village, Lvhua Township, Qianxi City, Guizhou province, China. The village has a total land area of 3.6 km^2, among them, 160.2 hm^2 of cultivated land, and 199.6 hm^2 of barren land (including 16.6 hm^2 of loess slope and 155.8 hm^2 rocky hill). Rocky desertification of local farmland is very common, and the major cash crops in Makan Village are chili, tobacco, and maize. The study area has a subtropical monsoon climate with clear wet and dry seasons. Droughts and water shortages are common during the winter and spring. The climate records from a local weather monitoring station show the mean annual temperature is 13.8 °C, fluctuating from the mean maximum temperature of 20.1 °C in July to the mean minimum temperature of 8.6 °C in January. Heavy rainfall and rainstorms become more frequent in the rainy season. The mean annual precipitation is 1049 mm, with approximately 80–88% occurring between May and October. The frequency of different rainfall intensities in annual precipitation is as follows: light rain ($p < 10$ mm) 22.2%, moderate rain ($10 \leq p < 25$ mm) 50.1%, heavy rain ($10 \leq p < 25$ mm) 19.4%, and torrential rain ($50 \leq p < 100$ mm) 8.3% [49].

The geomorphology of the study area is characterized by a typical karstic landscape, featuring variable microtopography shaped by rock outcrops. Upstanding rocks are scattered among the small patches of sloped cropland, and the rock outcrops are about one meter in height and shaped like a cone or triangular prism. The selected study plot (7.65% of slope) was located in a barren slope cropland, which has been uncultivated for years so that the topsoil structure and ground vegetation were not affected by agricultural activities and human disturbances. The soil is neutral and slightly acidic and belongs to brown lime soil and yellow lime soil, and the soil physical properties on the study site are shown in Table 1.

Table 1. Soil physical properties of the study site.

Soil Depth (cm)	Soil Particle Composition (%)			Soil Texture (USDA System)	Bulk Density (g·cm^{-3})	Capillary Porosity (%)
	2~0.05 mm	0.05~0.002 mm	<0.002 mm			
0~10	17.15	47.70	35.15	Silty clay loam	1.16 ± 0.13 b	46.92 ± 3.57 a
10~30	5.36	44.39	50.25	Silty clay	1.29 ± 0.36 a	41.36 ± 4.78 b

Notes: Data are expressed as mean ± SE. Different lowercase letters within rows indicate significant differences between plot types ($p < 0.05$).

2.2. Surface Runoff Collection

Ten soil–rock combination runoff plots were set in the study area; i.e., there were ten replicate groups. The selected soil–rock combinations were parallel to the slope in order to facilitate collecting surface runoff, and the collection devices of surface runoff were installed in soil patches surrounding rocks (Figure 1a). The sampling area of the soil patch was chosen so as to be neither too large nor too small, because too large an area would increase the difficulty of collecting the surface runoff, and too small an area would not reflect the actual characteristics of surface runoff in the karst zone. Firstly, a foam board was placed above the soil patch to form the upper boundary of the runoff plot to block surface runoff from above the slope. Secondly, a foam board was placed below the soil patch to form the

lower boundary of the runoff plot, and a water pipe with a filter and a water storage bag with a total capacity of 20 L were attached to this foam board. Finally, 3 rain gauges were placed in the plot to measure the cumulative rainfall of each rainfall event.

Figure 1. Design and implementation of the soil–rock combination runoff plot. (**a**) The placement of foam board, water storage bag, and rain gauge. (**b**) The projected area of the rock and the soil patch of the soil–rock combination runoff plot.

2.3. Measurement of Soil–Rock Catchment Area

The rainwater collecting area (i.e., projected area) of the rock and the soil patch in the runoff plots were measured by taking photographs (Figure 1b). The vegetation and litter were removed away from the soil surface before photographing. The ridge of the rock was painted white with chalk to facilitate the definition of the rock's projected area, and a scale ruler was placed on the ground to calibrate the photograph. And then, each runoff plot was shot vertically with a high-definition camera (Nikon D7200) at a height of 3 m. Finally, the projected area of the rock and the soil patch were measured using the software of Image J (V1.8.0.112). The projected areas of soil and rock of each soil–rock combination runoff plot were shown in Table 2.

Table 2. The projected areas of soil and rock of each soil–rock combination runoff plot.

Number	Rock Projected Area (cm^2)	Soil Projected Area (cm^2)	Total Projected Area (cm^2)
1	2575.35	1933.32	4508.67
2	4157.06	3283.01	7440.07
3	5615.44	5597.96	11,213.40
4	5833.86	9103.95	14,937.80
5	6849.43	5741.17	12,590.59
6	7401.53	7439.87	14,841.40
7	9244.61	7168.18	16,412.79
8	10,718.32	10,715.86	21,434.18
9	11,497.05	17,695.52	29,192.57
10	11,578.79	8722.13	20,300.92

2.4. Measurement of Soil Properties and Root Biomass

In order to analyze the influence of environmental factors on surface runoff generated by the soil patches, we measured the soil bulk density (g cm^{-3}), soil porosity (%), soil hydraulic conductivity (cm s^{-1}), and root biomass (Kg m^{-2}) for each runoff plot after the surface runoff measurements. Soil samples were randomly collected in three replications at depths of 0–30 cm with cutting cylinders (inner diameter 70.00 mm; height 52.00 mm; volume 200 cm^3). The soil core method was also used to measure the root biomass of plants within a soil depth of 0~20 cm in each runoff plot.

2.5. Statistical Analysis

All the data were tested for normality and homogeneity of variance. The normality of datasets was detected by the Shapiro–Wilk test, and homogeneity of variances was tested using Bartlett's test, prior to statistical analyses. A log transformation or square root transformation was conducted for non-normal distributions. Paired *t*-tests were used to compare the surface runoff yield among the different rainfall events. Significant differences between the means were detected based on the least significant difference (LSD) at $p < 0.05$.

To estimate the contribution of the rocks and the soils on the yield of surface runoff in the different rainfall events, multiple linear regression was used to analyze their respective rainfall–runoff conversion coefficient α (α_{rock} as the runoff coefficient of rocks and α_{soil} as the runoff coefficient of soils). We set the potential amount (mL) of rainwater received by rocks in a runoff plot (i.e., the rock area multiplied by rainfall) as an independent variable X, the potential amount (mL) of rainwater received by soils (i.e., the soil area multiplied by rainfall) as an independent variable Y, and the actual yield (mL) of surface runoff as the dependent variable Q. The relation function of the three variables is:

$$Q = X \times \alpha_{rock} + Y \times \alpha_{soil} \tag{1}$$

In order to verify the accuracy of the results, relationships between the calculated surface runoff yield (expressed as runoff depth, mm) produced by soils (i.e., R) and its influence factors (such as soil bulk density, soil porosity, soil hydraulic conductivity, and root biomass) under the different rainfall events were analyzed by Pearson correlation analysis. R was calculated as follows:

$$R = \frac{Q - X \times a_{rock}}{S} \times 10 \tag{2}$$

where the S is the projected area of soil in a runoff plot.

All statistical analyses were conducted using SPSS version 19.0 statistical software (SPSS Inc., Chicago, IL, USA). Figures were drawn using Origin 2022b.

3. Results

3.1. Surface Runoff Yield

During the rainy season, the yield (mL) of surface runoff collected from water storage bags in the sample plots was measured four times, and the results were shown in Figure 2a. The cumulative rainfall (consisting of continuous rainfalls or persistent rain showers) in the sample plot during the four measurement periods from large to small was 62 mm (torrential rain), 45 mm (heavy rain), 32 mm (heavy rain), and 19 mm (moderate rain) (Figure 3a), and the corresponding measured surface runoff depth was on average 2.53 mm, 1.46 mm, 0.77 mm, and 0.21 mm, respectively. Analysis of variance (ANOVA) showed that the surface runoff yield/depth under the different rainfall conditions was significantly different ($p < 0.05$). The surface runoff coefficient of the soil–rock runoff plots ranged from 0.0145 to 0.0408 on average with four rainfall events from small to large (Figure 3b).
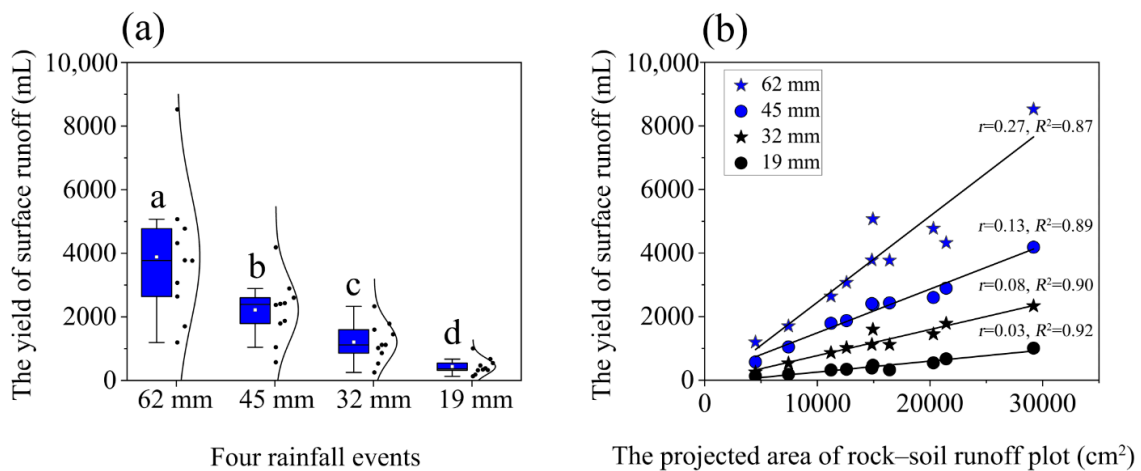
Figure 2. The yield of surface runoff (**a**) and its relationship with projected area of soil–rock runoff plots (**b**) under four different rainfall events. Different lowercase letters indicate significant differences among the groups ($p < 0.05$).
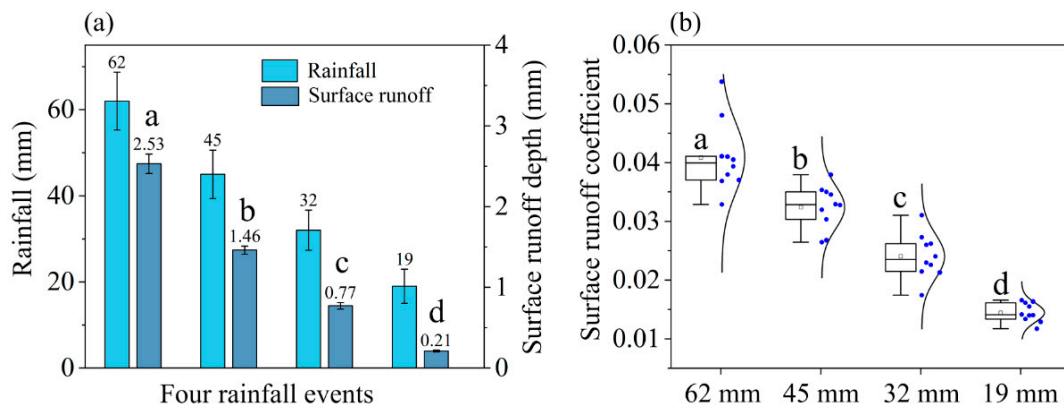
Figure 3. Surface runoff depth (**a**) and runoff coefficient of soil–rock combinations (**b**) under four different rainfall events. Different lowercase letters indicate significant differences among the groups ($p < 0.05$).

Surface runoff yield is positively correlated with the rainfall and the projected area of the rock–soil runoff plot (Figure 2b). Further, multiple regression analysis shows that (Figure 4) the α_{rock} and α_{soil} were different for the four different rainfall events, and the values of both increased with the increase in rainfall. The α_{rock} ranged from 0.004 to 0.015 and α_{soil} from 0.025 to 0.067 as the rainfall increased. The α_{soil} was always greater than the α_{rock} for every rainfall event, which means the soils' contribution to surface runoff yield was larger than that of the rocks.

3.2. Measurement Results of Environmental Factors

The measurement results of soil properties (0~30 cm depth) and root biomass (0~20 cm depth) of the ten selected soil–rock runoff plots were shown in Figure 5. Soil bulk density ranged from 1.19 to 1.36 g cm^{-3}. Soil porosity ranged from 43.71% to 50.09%, which was lower than that of the non-karst soils. Soil hydraulic conductivity ranged from 2.19×10^{-3} to 5.32×10^{-3} cm s^{-1}, and root biomass ranged from 0.13 to 0.21 kg m^{-2}. The results of the ten samples showed a normal distribution.
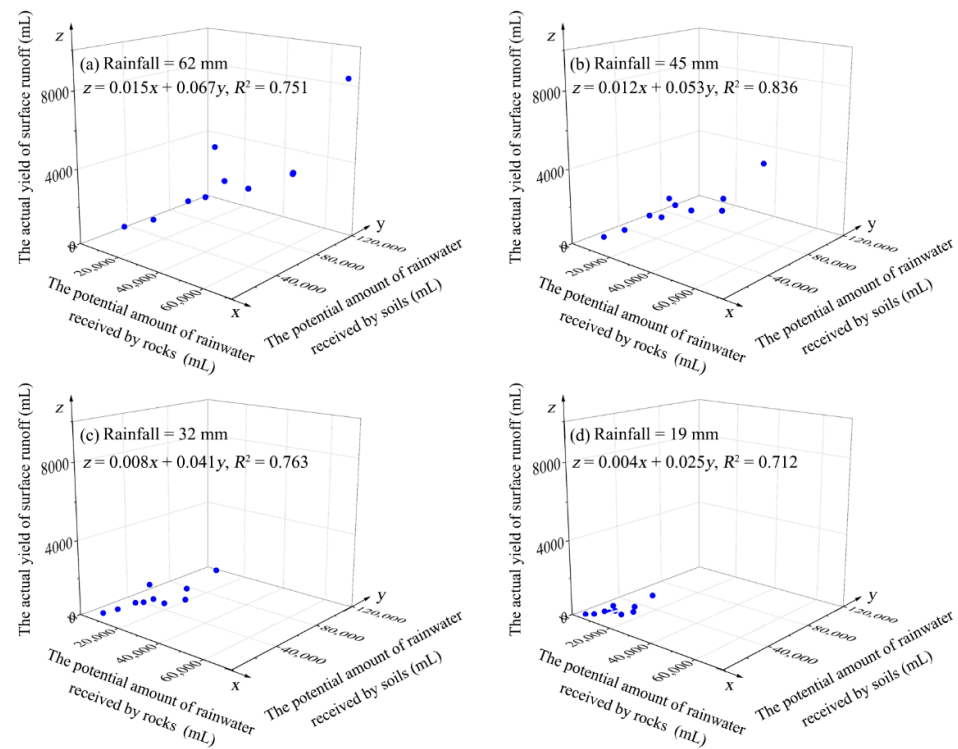
Figure 4. Multiple regression analysis of surface runoff yield for different rainfall events.
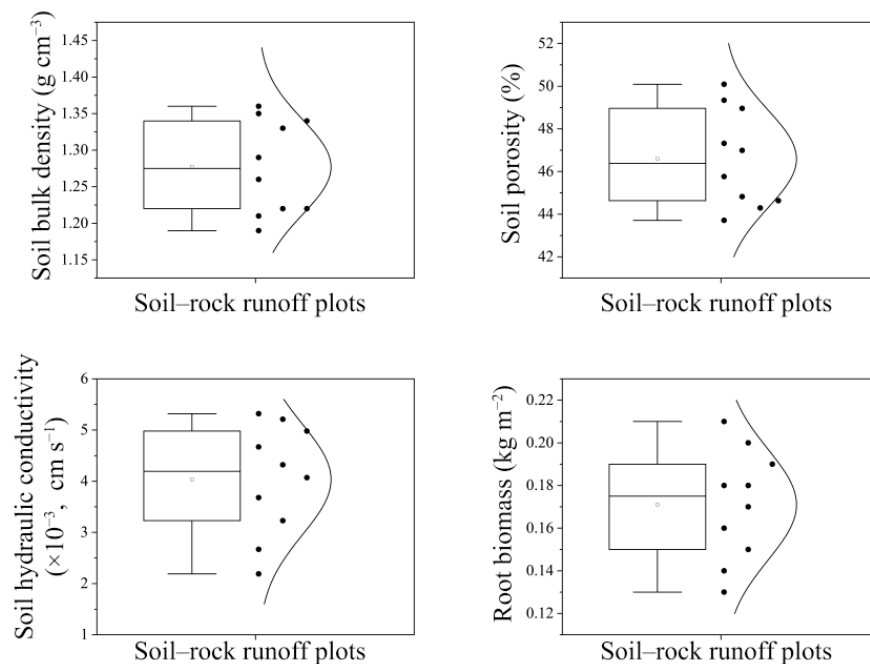

Figure 5. The soil properties and root biomass of the selected soil–rock runoff plots.

3.3. Correlation of R with Soil Properties and Root Biomass

Correlation analysis showed that the calculated *R* generally has a positive relationship with soil bulk density and a negative relationship with soil porosity, soil hydraulic conductivity, and root biomass (Table 3). The correlations from the four different measurements are increasingly significant with the increase in rainfall.

Table 3. Correlation coefficient of the calculated R with soil properties and root biomass under different rainfall events.
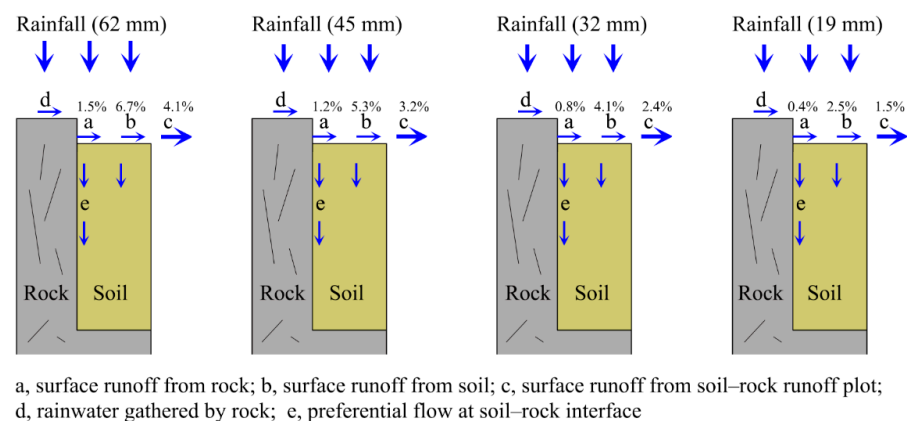
	Soil Bulk Density	Soil Porosity	Soil Hydraulic Conductivity	Root Biomass
$R_{62\ mm}$	0.739 *	−0.780 **	−0.812 **	−0.854 **
$R_{45\ mm}$	0.637 *	−0.875 **	−0.830 **	−0.719 *
$R_{32\ mm}$	0.641 *	−0.786 **	−0.885 **	−0.638 *
$R_{19\ mm}$	0.396	−0.321	−0.250	−0.235

Notes: R, surface runoff yield generated only from soils calculated based on Equation (2). * $p < 0.05$; ** $p < 0.01$.

4. Discussion

4.1. Characteristics of Surface Runoff in the Karst Area

This study showed that the coefficient of surface runoff in this area is very small, ranging from 0.0145 to 0.0408 in the measurement period (Figure 6). Obviously, this is because surface runoff on karst slope land is easy to be transformed into underground runoff, due to the unique aboveground and underground dual hydrological structure [50,51]. It has been suggested that the "mosaic" pattern of soil–rock microgeomorphic units represents the strong spatial heterogeneity of the land surface, and the rock barrier affects the continuity of surface runoff, increasing the contact time between the surface water and the soil [28,40]. The existence of surface rocks, therefore, increases the infiltration of soil water and results in a much lower runoff coefficient in the karst area than in other areas, such as the Loess plateau, further causing underground leakage and aggravating rocky desertification-derived drought [50,51]. More importantly, surface runoff processes, as an important part of the terrestrial water cycle, can affect a series of ecological processes such as groundwater recharge and water balance in karst areas. This study proved that the area has abundant rainfall, but because of the small surface runoff coefficient caused by the shallow soil layer's low water storage capacity and strong karstification, surface water is easily transported vertically to the bedrock, then lost through cracks and pipes. The karst groundwater system, therefore, has unique characteristics of hydrogeochemical and prominent geochemical vulnerability and environmental frangibility.

a, surface runoff from rock; b, surface runoff from soil; c, surface runoff from soil–rock runoff plot;
d, rainwater gathered by rock; e, preferential flow at soil–rock interface

Figure 6. Rainfall–runoff relationship of karst slope under different rainfall events.

In this study, the runoff coefficient showed a significant positive correlation with rainfall, which is consistent with previous findings [52–54]. Guizhou province has a subtropical monsoon climate with high precipitation and low regional evaporation, and there is plenty of rainwater feeding the rocky desertification area with rainfall averaging approximately 1100–1300 mm yr^{-1}. While some studies have reported that rainfall is one of the main driving forces of soil erosion and rocky desertification in karst areas, and rainfall intensity is the most important factor affecting slope erosion and sediment yield [53,54],

substantial increase in the surface runoff coefficient does not easily occur in karst areas (especially rocky desertification areas) less affected by human activities, despite the fact that the coefficient of surface runoff increases synchronously with the variation of rainfall in this study. It has been suggested that the soil–rock geomorphic unit is the cause of the uneven distribution of rainfall and surface runoff and is also the key factor that results in the complicated process and mechanism of groundwater transport in the karst area, which has good effects on rainfall–runoff regulation and control (Figure 6). When rainfall reaches a certain level, after the vegetation interception and the soil water content are saturated, the excess rainwater can be lost not only through surface runoff but also through the soil–rock interface, quickly leaking into the ground, thus reducing soil loss.

4.2. The Influence Factors of Surface Runoff

Our results showed that the precipitation, geomorphic units, soil, and vegetation will greatly affect slope runoff. Rainfall is the basis of surface runoff on slopes, and surface runoff yield is the reaction of various natural factors. The surface hydrological process is affected by the characteristics of land cover, especially in karst areas, where the rocky desertification area has a strong influence on rainfall redistribution, infiltration, and surface runoff [28,44]. Despite the general significance of saturation-excess and infiltration-excess runoff in the karst basin, there are still large gas-phase structures under the surface causing a relatively complex runoff mechanism. Surface runoff in karst areas is a multifactorial process that is influenced and regulated by a combination of environmental and internal factors [22]. The distribution of exposed carbonate rocks and shallow soil divides the land into a varied pattern, and the process of soil water transport becomes more complex with this geological background.

In areas with many outcropping rocks, the voids between the exposed rock and the surrounding soil make the rock–soil interface the main preferred flow path for soil water infiltration [4,26,28], and the huge amount of rocks extending from the surface to the underground bedrock can affect the infiltration of soil water and the surface runoff processes. When rainfall is intercepted by rocks to form rock surface flow, most rock surface flows might penetrate into deep soil along the preferential channel of the soil–rock interface, and only a small part merges into surface runoff, which is consistent with the study of Sohrt et al. [26] that runoff generated by rainfall on bare rock surface rarely participates in surface runoff. The permeability of soil surrounding rocks is extremely high, even greater than the general natural rainfall intensity of the areas, which leads to little saturation-excess runoff on karst slopes. Only under exceptional circumstances such as heavy rains or severe soil crusts is the runoff from rocks likely to exceed the permeability of the soil and spread laterally to soil patches by infiltration-excess runoff [26,28]. Nonetheless, the rocks as barriers hinder the continuity of surface runoff in most cases, and tortuous flow paths undoubtedly increase the contact time between surface runoff and the soil, leading to another vertical permeability and the reduction of surface runoff. In our study, the surface runoff coefficient of rocks was smaller than that of soil, which means rocks contribute less to the yield of surface runoff than the soil of the same area. This supports the idea, promulgated by some researchers [22,44,55], that the yield of surface runoff gradually decreases with an increase of surface rock coverage.

In addition to the external influences of rocks, there are the added internal factors, such as soil bulk density, soil porosity, soil hydraulic conductivity, and soil root biomass, that affect the surface runoff yield in this study. Soil surface composition is an important factor in controlling surface runoff, and studies have found that when a soil crust develops, surface sealing will increase, and water channels in the soil will be blocked, finally resulting in a reduction of vertical infiltration and an increase in surface runoff [44,55]. This is also confirmed by our experimental data which show a positive correlation between the calculated R and soil bulk density, alongside a negative correlation with soil porosity and soil hydraulic conductivity (Table 3). The clay content of karst soil is so high that soil crusting is very common, which might lead to low soil hydraulic conduction and promote

surface runoff. However, because of the thin solum and well-developed preferential flow, the surface runoff coefficient in the karst area is actually much smaller than in other areas, as the study results suggested (Figure 3b). In addition, the negative correlation between the calculated R and root biomass suggested that non-soil components such as plant roots and litter can reduce soil density and increase soil water penetration rates. As an aside, the fauna living in the soil can also affect surface runoff because the burrows they produce effectively increase soil porosity, and soil cracks formed during drought in karst areas can provide a preferred path of soil water flow, promoting deep seepage of surface soil water and reducing the surface runoff coefficient [28,56].

4.3. Application

The relationships between the calculated R and its influence factors are in good agreement with previous studies based on traditional runoff plots [22,25,44,52,53], which demonstrated the accuracy and efficiency of the proposed method in our study. There have been many tests focusing on the monitoring and measurement of surface runoff yield on karst slopes, but the results obtained in different regions are variable, and the differences among them are large because the surface runoff process in karst areas is strongly dominated by the geological environment. The area, boundary, and reservoir of runoff plots are important factors that affect the results of surface runoff research. In this study, the soil–rock combination geomorphic units were defined as the runoff plot with rocks as the left or/and right boundary walls, and a water storage bag was used to collect runoff to avoid evaporation. These measures can make up for the shortage of traditional runoff plots and, to a certain extent, the experimental error can be reduced. The measuring technique and application of runoff plots for soil erosion and surface runoff in this region is a key problem to be solved in regional ecological construction. The proposed method in our study is helpful to understand the rainfall–runoff process of a karst slope and to estimate the yield of surface runoff, and thus it might provide some food for thought for the prevention and treatment measures of soil water loss in karst zones.

One of the effective measures to prevent soil erosion is to legitimately manage and control surface runoff. The surface runoff caused by rainfall is a significant driving force for soil erosion on karst slopes [52,54], and thus rocks can help decrease soil loss to some extent based on their small contribution to surface runoff. By studying the influence of rocks and soil under different rainfall conditions, it has been found that the contribution of rocks to surface runoff is smaller than that of soils. The surface runoff coefficient is very low in rocky desertification areas because of the widely distributed rocks, which leads to rapid loss of water resources such as surface runoff and subsurface runoff, so soil erosion caused by runoff can be avoided on a huge scale. In practice, eradicating rocks from the surface to control rocky desertification can increase the area of arable land, but the surface runoff coefficient of the land will be increased invisibly, eventually leading to soil erosion increasing and rocky desertification aggravating. Surface rock is a common element of karst landscapes having a specific ecological significance and function [27,38,39,57,58], and future studies should pay more attention to the ecohydrological effects of surface rocks, such as the funneling effect on rainfall, the blocking (or retarding) effect on surface runoff, and the mosaic effect of the rock–soil combination on the hydrological process.

5. Conclusions

Through monitoring rainfall runoff by soil–rock runoff plots under different rainfall events, it has been proven that the coefficient of surface runoff measured on uncultivated land of a karst area is very small compared to that of non-karst areas. And multiple regression analysis showed that the rocks contributed less to the yield of surface runoff than the soils, and with the increase in rainfall, the contributions of both showed an increasing trend. The calculated R showed a positive relationship with soil bulk density and a negative relationship with soil porosity, soil hydraulic conductivity, and root biomass. These study results contribute to a deeper understanding of the rainfall–runoff process in

rocky desertification areas, and the proposed method of the soil–rock runoff plot provides a new way to estimate the yield of rainfall runoff on the complicated geomorphic units of karst slopes.

References

1. Green, S.M.; Dungait, J.A.J.; Tu, C.L.; Buss, H.L.; Sanderson, N.; Hawkes, S.J.; Xing, K.X.; Yue, F.J.; Hussey, V.L.; Peng, J.; et al. Soil functions and ecosystem services research in the Chinese karst critical zone. *Chem. Geol.* **2019**, *527*, 119107. [CrossRef]

2. Xiao, W.J.; Yang, Y.; Jiang, X.Y.; He, Z.L.; Zou, X.G.; You, X.H.; Yang, Y.Y.; Zeng, Z.Z.; Shi, W.Y. Differentresponses of ecohydrologi-calprocesses in the re-vegetationarea between the dip and anti-dip slope in a karst rockydesertification area in southwestern China. *Plant Soil* **2021**, *475*, 25–43. [CrossRef]

3. Xiong, K.N.; Zhang, R.K.; Liu, Z.Q.; Lyu, X.; Hu, C.P. A review of nitrogen export and its eco-environmental significance in the superficial karst desertification zone. *Water* **2023**, *15*, 1864. [CrossRef]

4. Zhao, Z.M.; Wang, Q.H. Effect of rock film mulching on preferential flow at rock–soil interfaces in rocky karst areas. *Water* **2023**, *15*, 1775. [CrossRef]

5. Husic, A.; Fox, J.; Adams, E.; Ford, W.; Agouridis, C.; Currens, J.; Backus, J. Nitrate pathways, processes, and timing in an agricultural karst system: Development and application of a numerical model. *Water Resour. Res.* **2019**, *55*, 2079–2103. [CrossRef]

6. Qin, L.Y.; Bai, X.Y.; Wang, S.J.; Zhou, D.Q.; Li, Y.; Peng, T.; Tian, Y.C.; Luo, G.J. Major problems and solutions on surface water resource utilisation in karst mountainous areas. *Agric. Water Manag.* **2015**, *159*, 55–65. [CrossRef]

7. Smith, D.N.I.; Ortega-Camacho, D.; Acosta-Gonzalez, G.; Leal-Bautista, R.M.; Fox, W.E.; Cejudo, E. A multi-approach assessment of land use effects on groundwater quality in a karstic aquifer. *Heliyon* **2020**, *6*, e03970. [CrossRef] [PubMed]

8. Liu, J.C.; Shen, L.C.; Wang, Z.X.; Duan, S.H.; Wu, W.; Peng, X.Y.; Wu, C.; Jiang, Y.J. Response of plants water uptake patterns to tunnels excavation based on stable isotopes in a karst trough valley. *J. Hydrol.* **2019**, *571*, 485–493. [CrossRef]

9. Koit, O.; Barbera, J.A.; Marandi, A.; Terasmaa, J.; Kiivit, I.K.; Martma, T. Spatiotemporal assessment of humic substance-rich stream and shallow karst aquifer interactions in a boreal catchment of northern Estonia. *J. Hydrol.* **2020**, *580*, 124238. [CrossRef]

10. Peng, X.D.; Dai, Q.H.; Ding, G.J.; Li, C.L. Role of underground leakage in soil, water and nutrient loss from a rock-mantled slope in the karst rocky desertification area. *J. Hydrol.* **2019**, *578*, 124086. [CrossRef]

11. Zhou, Q.W.; Luo, Y.; Zhou, X.; Cai, M.Y.; Zhao, C.W. Response of vegetation to water balance conditions at different time scales across the karst area of southwestern China—A remote sensing approach. *Sci. Total Environ.* **2018**, *645*, 460–470. [CrossRef]

12. Zhu, X.R.; Liu, H.Y.; He, W.Q.; Wu, L.; Liu, F. Regolith water storage patterns determine vegetation productivity in global karst regions. *Geoderma* **2023**, *430*, 116292. [CrossRef]

13. Huang, K.; Wang, R.; Wu, W.X.; Wu, P.L.; Li, H.X.; Zeng, L.L.; Shao, J.H.; Liu, H.C.; Xu, T. Trend of vegetation and environmental factors and their feedback in the karst regions of southwestern China. *Sustainability* **2022**, *14*, 15941. [CrossRef]

14. Ning, J.; Liu, X.; Wu, X.; Yang, H.; Ma, J.; Cao, J.H. The effect of bedrock differences on plant water use strategies in typical karst areas of southwest China. *Land* **2023**, *12*, 12. [CrossRef]

15. Li, Y.Q.; Jiang, Z.C.; Chen, Z.H.; Yu, Y.; Lan, F.; Shan, Z.J.; Sun, Y.J.; Liu, P.; Tang, X.B.; Rodrigo-Comino, J. Anthropogenic disturbances and precipitation affect karst sediment discharge in the Nandong underground river system in Yunnan, southwest China. *Sustainability* **2020**, *12*, 3006. [CrossRef]

16. Zhu, D.Y.; Xiong, K.N.; Xiao, H. Multi-time scale variability of rainfall erosivity and erosivity density in the karst region of southern China, 1960–2017. *Catena* **2021**, *197*, 104977. [CrossRef]

17. Adji, T.N.; Haryono, E.; Mujib, A.; Fatchurohman, H.; Bahtiar, I.Y. Assessment of aquifer karstification degree in some karst sites on Java Island, Indonesia. *Carbonates Evaporites* **2019**, *34*, 53–66. [CrossRef]

18. Calaforra, J.M.; Pulido-Bosch, A. Evolution of the gypsum karst of Sorbas (SE Spain). *Geomorphology* **2003**, *50*, 173–180. [CrossRef]
19. Zhao, Z.M.; Shen, Y.X. Rain-induced weathering dissolution of limestone and implications for the soil sinking-rock outcrops emergence mechanism at the karst surface: A case study in southwestern China. *Carbonates Evaporites* **2022**, *37*, 69. [CrossRef]
20. Tao, S.; Zhang, L.K.; Liu, P.Y.; Zou, S.Z.; Yi, Z.; Xiang, L.; Li, D.Y. Transformation process of five water in epikarst zone: A case study in subtropical karst area. *Environ. Earth Sci.* **2022**, *81*, 293. [CrossRef]
21. Zhao, Y.M.; Liao, W.H.; Lei, X.H. Hydrological simulation for karst mountain areas: A case study of central Guizhou province. *Water* **2019**, *11*, 991. [CrossRef]
22. Dai, Q.H.; Peng, X.D.; Yang, Z.; Zhao, L.S. Runoff and erosion processes on bare slopes in the karst rocky desertification area. *Catena* **2017**, *152*, 218–226. [CrossRef]
23. He, J.H.; Cao, Y.; Zhang, K.L.; Xiao, S.Z.; Cao, Z.H. Soil loss through fissures and its responses to rainfall based on drip water monitoring in karst caves. *J. Hydrol.* **2023**, *617*, 129000. [CrossRef]
24. Li, G.J.; Rubinato, M.; Wan, L.; Wu, B.; Luo, J.F.; Fang, J.M.; Zhou, J.X. Preliminary characterization of underground hydrological processes under multiple rainfall conditions and rocky desertification degrees in karst regions of southwest China. *Water* **2020**, *12*, 594. [CrossRef]
25. Peng, X.D.; Dai, Q.H.; Li, C.L.; Zhao, L.S. Role of underground fissure flow in near-surface rainfall-runoff process on a rock mantled slope in the karst rocky desertification area. *Eng. Geol.* **2018**, *243*, 1017. [CrossRef]
26. Sohrt, J.; Ries, F.; Sauter, M.; Lange, J. Significance of preferential flow at the rock soil interface in a semi-arid karst environment. *Catena* **2014**, *123*, 1–10. [CrossRef]
27. Zhao, Z.M.; Shen, Y.X.; Shan, Z.J.; Yu, Y.; Zhao, G.J. Infiltration patterns and ecological function of outcrop runoff in epikarst areas of southern China. *Vadose Zone J.* **2018**, *17*, 1–10. [CrossRef]
28. Zhao, Z.M.; Shen, Y.X.; Jiang, R.H.; Wang, Q.H. Rock outcrops change infiltrability and water flow behavior in a karst soil. *Vadose Zone J.* **2020**, *19*, e20002. [CrossRef]
29. Mitra, S.; Singh, S.; Srivastava, P. Sensitivity of groundwater components to irrigation withdrawals during droughts on agricultural-intensive karst aquifer in the Apalachicola-Chattahoochee-Flint River Basin. *J. Hydrol. Eng.* **2019**, *24*, 05018032. [CrossRef]
30. Mitra, S.; Srivastava, P.; Singh, S. Effect of irrigation pumpage during drought on karst aquifer systems in highly agricultural watersheds: Example of the Apalachicola-Chattahoochee-Flint river basin, southeastern USA. *Hydrogeol. J.* **2016**, *24*, 1565–1582. [CrossRef]
31. Singh, S.; Mitra, S.; Srivastava, P.; Abebe, A.; Torak, L. Evaluation of water-use policies for baseflow recovery during droughts in an agricultural intensive karst watershed: Case study of the lower Apalachicola-Chattahoochee-Flint River Basin, southeastern United States. *Hydrol. Process.* **2017**, *31*, 3628–3644. [CrossRef]
32. Chen, S.L.; Xiong, L.H.; Zeng, L.; Kim, J.S.; Zhang, Q.; Jiang, C. Distributed rainfall-runoff simulation for a large-scale karst catchment by incorporating landform and topography into the DDRM model parameters. *J. Hydrol.* **2022**, *610*, 127853. [CrossRef]
33. Gregory, L.; Wilcox, B.P.; Shade, B.; Munster, C.; Owens, K.; Veni, G. Large-scale rainfall simulation over shallow caves on karst shrublands. *Ecohydrology* **2009**, *2*, 72–80. [CrossRef]
34. Vilhar, U.; Kermavnar, J.; Kozamernik, E.; Petric, M.; Ravbar, N. The effects of large-scale forest disturbances on hydrology—An overview with special emphasis on karst aquifer systems. *Earth-Sci. Rev.* **2022**, *235*, 104243. [CrossRef]
35. Fonseca, M.R.S.; Uagoda, R.E.S.; Chaves, H.M.L. Runoff, soil loss, and water balance in a restored Karst area of the Brazilian Savanna. *Catena* **2023**, *222*, 106878. [CrossRef]
36. Kang, X.B.; Luo, S.; Xu, M. Research on the mechanism of water resource loss in east karst mountain area of Sichuan. *Desalin Water Treat.* **2015**, *53*, 557–566. [CrossRef]
37. Wang, Z.H.; Luo, D.; Xiong, K.N.; Gu, X.; Zhu, Z.Z. Studies on hydrological processes on karst slopes for control of soil and water loss. *Sustainability* **2022**, *14*, 5789. [CrossRef]
38. Shen, Y.X.; Wang, D.J.; Chen, Q.Q.; Tang, Y.Y.; Chen, F.J. Large heterogeneity of water and nutrient supply derived from runoff of nearby rock outcrops in karst ecosystems in SW China. *Catena* **2019**, *172*, 125–131. [CrossRef]
39. Shen, Y.X.; Wang, Q.H.; Zhao, Z.M.; Yuan, C. Fine-scale effect of karst rock outcrops on adjacent soil and plant communities in Southwest China. *Catena* **2022**, *219*, 106592. [CrossRef]
40. Zhao, Z.M.; Shen, Y.X.; Wang, Q.H.; Jiang, R.H. The temporal stability of soil moisture spatial pattern and its influencing factors in rocky environments. *Catena* **2020**, *187*, 104418. [CrossRef]
41. Wang, D.J.; Shen, Y.X.; Huang, J.; Li, Y.H. Rock outcrops redistribute water to nearby soil patches in karst landscapes. *Environ. Sci. Pollut. R.* **2016**, *23*, 8610–8616. [CrossRef]
42. Yang, W.; Peng, X.D.; Dai, Q.H.; Li, C.L.; Xu, S.B.; Liu, T.T. Storage infiltration of rock-soil interface soil on rock surface flow in the rocky desertification area. *Geoderma* **2023**, *435*, 116512. [CrossRef]
43. Wang, F.; Chen, H.S.; Lian, J.J.; Fu, Z.Y.; Nie, Y.P. Preferential flow in different soil architectures of a small karst catchment. *Vadose Zone J.* **2018**, *17*, 180107. [CrossRef]
44. Li, X.Y.; Contreras, S.; Sole-Benet, A.; Canton, Y.; Domingo, F.; Lazaro, R.; Lin, H.; Van Wesemael, B.; Puigdefabregas, J. Controls of infiltration-runoff processes in Mediterranean karst rangelands in SE Spain. *Catena* **2011**, *86*, 98–109. [CrossRef]
45. Fu, T.G.; Chen, H.S.; Zhang, W.; Nie, Y.P.; Gao, P.; Wang, K.L. Spatial variability of surface soil saturated hydraulic conductivity in a small karst catchment of southwest China. *Environ. Earth Sci.* **2015**, *74*, 2381–2391. [CrossRef]

46. Yang, J.; Xu, X.L.; Liu, M.X.; Xu, C.H.; Luo, W.; Song, T.Q.; Du, H.; Kiely, G. Effects of Napier grass management on soil hydrologic functions in a karst landscape, southwestern China. *Soil Till. Res.* **2016**, *157*, 83–92. [CrossRef]

47. Han, Z.; Yang, X.C.; Yin, X.A.; Fang, Q.; Zhao, L.S. Effect of exposed roots on the erosion characteristics of sloped land based on close-range photogrammetry in a karst rocky desertification region. *Catena* **2023**, *225*, 107035. [CrossRef]

48. Wang, S.J.; Liu, Q.M.; Zhang, D.F. Karst rocky desertification in southwestern China: Geomorphology, landuse, impact and rehabilitation. *Land Degrad. Dev.* **2004**, *15*, 115–121. [CrossRef]

49. Pan, L.D.; Li, R.; Li, Q.G. Huang Kai Zhang Linqing Effects of Straw Mulching on Runoff and Sediment Characteristics of Sloping Farmland in the Karst Area of Western Guizhou. *J. Soil Water Conserv.* **2021**, *35*, 9–16. (In Chinese)

50. Fan, C.H.; Zhao, L.S.; Hou, R.; Fang, Q.; Zhang, J.X. Quantitative analysis of rainwater redistribution and soil loss at the surface and belowground on karst slopes at the microplot scale. *Catena* **2023**, *227*, 107113. [CrossRef]

51. Fang, Q.; Zhao, L.S.; Hou, R.; Fan, C.H.; Zhang, J.X. Rainwater transformation to runoff and soil loss at the surface and belowground on soil-mantled karst slopes under rainfall simulation experiments. *Catena* **2022**, *215*, 106316. [CrossRef]

52. Liu, W.; Li, Z.W.; Zhu, J.X.; Xu, C.H.; Xu, X.L. Dominant factors controlling runoff coefficients in karst watersheds. *J. Hydrol.* **2020**, *590*, 125486. [CrossRef]

53. Wang, S.; Yan, Y.; Fu, Z.Y.; Chen, H.S. Rainfall-runoff characteristics and their threshold behaviors on a karst hillslope in a peak-cluster depression region. *J. Hydrol.* **2022**, *605*, 127370. [CrossRef]

54. Zhao, L.S.; Fang, Q.; Hou, R.; Wu, F.Q. Effect of rainfall intensity and duration on soil erosion on slopes with different microrelief patterns. *Geoderma* **2021**, *396*, 115085. [CrossRef]

55. Juan, J.; Liu, D.D.; Fei, Y.H.; Pu, L. Combined effects of moss colonization and rock fragment coverage on sediment losses, flow hydraulics and surface microtopography of carbonate-derived laterite from karst mountainous lands. *Catena* **2023**, *229*, 107202. [CrossRef]

56. Hou, F.; Cheng, J.H.; Guan, N. Investigating the effect of soil cracks on preferential flow using a dye tracing infiltration experiment in karst in Southwest China. *Land Degrad. Dev.* **2023**, *34*, 1612–1628. [CrossRef]

57. Luo, L.; Wu, Y.Y.; Li, H.T.; Xing, D.K.; Zhou, Y.; Xia, A.T. Drought Induced Dynamic Traits of Soil Water and Inorganic Carbon in Different Karst Habitats. *Water* **2022**, *14*, 3837. [CrossRef]

58. Luo, Y.; Shi, C.M.; Yang, S.T.; Liu, Y.; Zhao, S.; Zhang, C.C. Characteristics of soil calcium content distribution in karst dry-hot valley and its influencing factors. *Water* **2023**, *15*, 1119. [CrossRef]